

# Study of Clutter Influence on a Differential BPSK Decoder, Providing a Minimal Intersymbol Interference

Georgi V. Stanchev<sup>1</sup> and Marin S. Marinov<sup>2</sup>

**Abstract**– This paper studies both Doppler shift and additive white Gaussian noise influence on a differential BPSK decoder which includes matched filters in its in-phase and quadrature channels. Results about probability density function of the output signal and probability of error at the output are obtained.

**Keywords**– differential BPSK decoder, minimal inter-symbol interference, matched filter, phase difference rejection, Doppler shift, AWGN.

## I. INTRODUCTION

The mobile communication channels suffer from additional influences in comparison with the wire channels. Some of them are Doppler shift, high level noise and multipath. These phenomena and to be more precise their stochastic nature makes equipment performance estimation difficult to access. But in present days with the frequency spectrum overloading and object speed increasing, the demands and requirements to service quality of communications in mobile environment grow, too. Realistic and practical applicable results can be obtained only if the joint clutter influence of the damaging factors and technical limits are considered together.

Here the performance of a differential BPSK decoder, described in [2], suffering from clutter influence of Doppler shift and additive white Gaussian noise (AWGN) is researched. The single path propagation of the signal through the radio-channel is presupposed.

## II. SIGNAL PROCESSING IN THE RECEIVER

The mixture of a useful digital modulated signal  $r(t)$  and AWGN at the front end of the receiver is described as:

$$r(t) = R(t)\cos(\omega_0 t) + n_G(t). \quad (1)$$

The diagram shown in Fig.1 describes the main elements of the signal processing in the receiver.

The receiver design in any case requires the frequency band of the receiver to be limited and this is taken into account by band-pass filter (BPF) including. In this manner the noise after BPF can be described as a narrow-band process:

$$r(t) = [R(t) + n(t)]\cos(\omega_0 t). \quad (2)$$

The Doppler shift is introduced by a frequency offset  $\omega_D$  of the receiver local oscillator. In this manner frequency recovery inaccuracies can be marked, too.

The results from down converting in the in-phase I-channel and quadrature Q-channel are:

$$\begin{aligned} R_I(t) &= [R(t) + n(t)]\{\cos(\omega_D t + \psi) + \cos[(2\omega_0 + \omega_D)t + \psi]\}, \\ R_Q(t) &= [R(t) + n(t)]\{\sin(\omega_D t + \psi) + \sin[(2\omega_0 + \omega_D)t + \psi]\}. \end{aligned} \quad (3)$$

The matched filters are low-passed filters by nature and hence they reject the components around doubled carrier frequency effectively. The signals at the filter outputs are:

$$\begin{aligned} S_I(t) &= R_I(t) * H(t) \approx \{[R(t) + n(t)]\cos(\omega_D t + \psi)\} * H(t); \\ S_Q(t) &= R_Q(t) * H(t) \approx \{[R(t) + n(t)]\sin(\omega_D t + \psi)\} * H(t). \end{aligned} \quad (4)$$

These signals are sampled in order to reject the intersymbol interference and then they are differentially decoded.

## III. RESEARCHES

The studies of the decoder, which is described above, in presence of Doppler shift show that the influence of Doppler shift is hardly seen and there is no need to take it in account, when practical system is considered – Globalstar for example.

Studies of the output signal distribution at different values of signal to noise ratio (SNR) are done. In [1] is shown that the energy of signal is equal to the chip duration value  $T_C$ . This value is used in order to calculate the variance of the continuous AWGN. When the noise is simulated this one is a discrete process and its variance is related to that of continuous process by the Eq. 5:

$$\sigma_d^2 = \frac{\sigma^2}{\Delta t}, \quad (5)$$

where  $\Delta t = \pi/\omega_0$  is the sampling period.

In order to obtain results about the distribution of the output signal at each SNR 10 000 realizations are used. The values of the window width and the roll-off factor are chosen in keeping with recommendations produced in [2]. Enough statistics is provided by rounding off to 0.02 of the output signal values. The designed software uses numerical integration in order to calculate the convolution between the input signals and impulse responses of the matched filters in both of quadrature channels. The frequency of occurrence for each output signal value at concrete SNR is calculated. Actually it is the distribution of the output signal. Some of the results are presented in the following figures

The output signal distributions at values of 1 and 3 for the roll-off factor and the relative window width respectively are shown in Fig.2.

<sup>1</sup>Georgi V. Stanchev, PhD is with the Aviation Faculty, National Military University, 5856 Dolna Mitropolia, Bulgaria, e-mail: gstanchev@af-acad.bg.

<sup>2</sup>Marin S. Marinov, PhD is with the Aviation Faculty, National Military University, 5856 Dolna Mitropolia, Bulgaria, e-mail: mmarinov2000@yahoo.com.

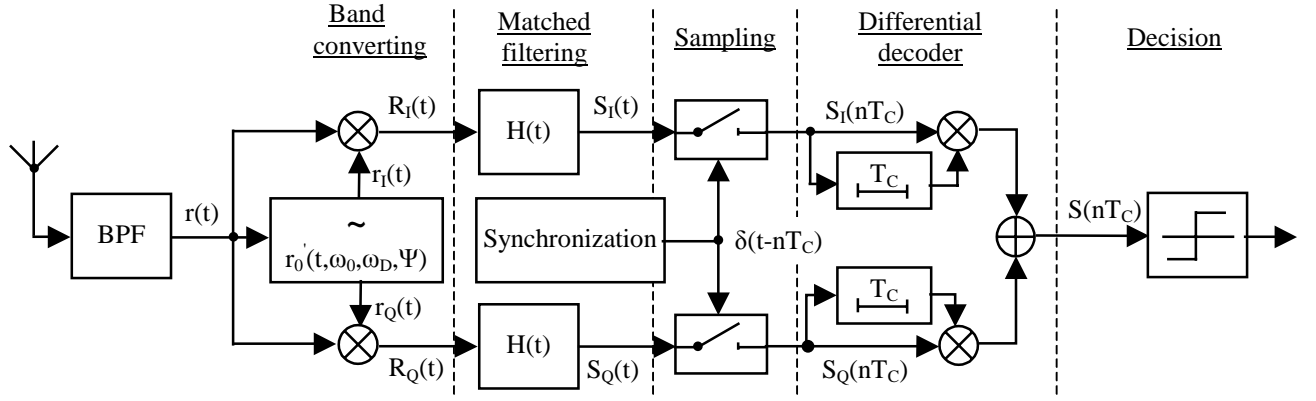


Fig.1 Model of the receiver.

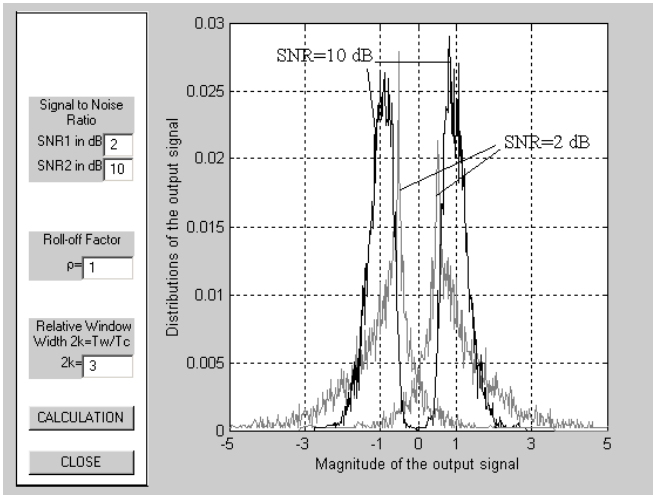


Fig.2. Distributions of output signal at  $\rho=1$  and  $2k=3$ .

The results show that the lower SNR leads to a wider output signal distribution. The values with the highest frequency of occurrence are far enough from zero even at SNR of 2 dB. It is obvious that the distribution at SNR of 10 dB is much narrower than this one at 2 dB. The values with the highest frequency of occurrence are closer to -1 and +1 respectively at the higher SNR.

Many more than 10 000 realizations are needed to calculate the probability of error. This is unpractical because too much time would be wasted to obtain results. It is advisable to approximate the probability density function (PDF) of output signal by using its distribution obtained from realizations.

In case of Gaussian channel the distribution of output signal possesses a Gaussian (normal) distribution. The normal probability density function is given by:

$$p(S) = \frac{1}{\sqrt{2\pi\sigma}} \exp\left\{-\frac{(S-m)^2}{2\sigma^2}\right\}, \quad (6)$$

where  $m$  is the mean value and  $\sigma^2$  is the variance. This is the continuous distribution and it is used in order to obtain the discrete distribution by next equation:

$$P(S_i) = \int_{S_i - \Delta S/2}^{S_i + \Delta S/2} p(S) dS, \quad (7)$$

where  $S_i$  are the discrete values of the output signal and  $\Delta S$  is the discrete step between two adjacent values.

The integral of normal probability density function in Eq.7 can be solved by means of famous error function [3]:

$$\text{erf}(S) = \frac{2}{\sqrt{\pi}} \int_0^S \exp\{-x^2\} dx. \quad (8)$$

The discrete distribution is derived from Eq.7 and Eq.8:

$$P(S_i) = \frac{1}{2} \left[ \text{erf}\left(\frac{S_i + \Delta S/2}{\sqrt{2}\sigma}\right) - \text{erf}\left(\frac{S_i - \Delta S/2}{\sqrt{2}\sigma}\right) \right]. \quad (9)$$

The optimal mean value  $m$  and the root mean square  $\sigma$  at which the equation (9) best fits the obtained distribution of the output signal are calculated. Then they are substituted in (6) and the probability density functions which best fit to the output signal distribution are obtained.

The approximated probability density functions of output signal at values of the roll-off factor 1 and the relative window width 3 are shown in Fig.3.

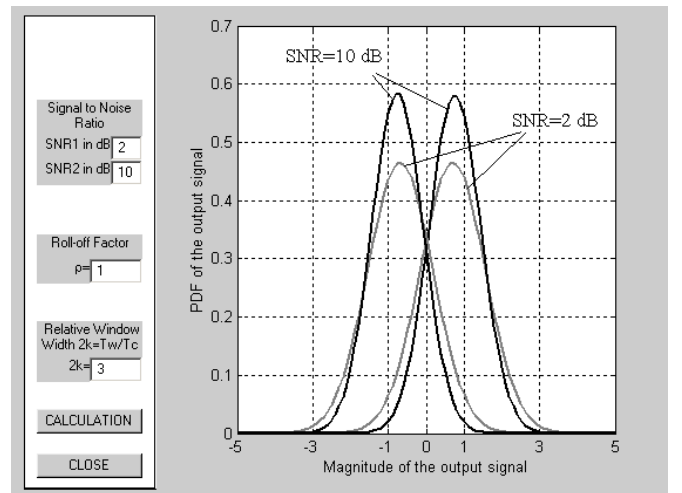


Fig.3. PDF of the output signal at  $\rho=1$  and  $2k=3$ .

It is clearly seen that the probability for output signal to exceed zero, when -1 is transmitted, is higher at lower SNR. The probability for output signal to be below zero, when +1 is transmitted, is higher at lower SNR, too. These two cases determine the error level at the decoder output.

The distributions of the output signal at values of 0.5 and 6 for the roll-off factor and the relative window width respectively are shown in Fig.4.

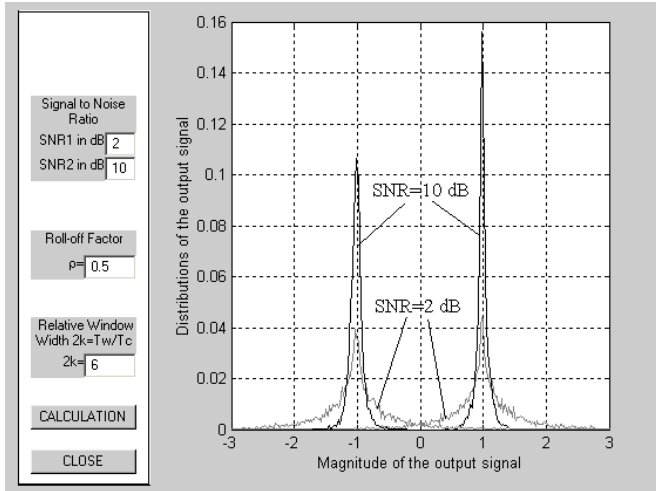


Fig.4. Distributions of the output signal at  $\rho=0.5$  and  $2k=6$ .

The results show that the distribution of output signal in this case is narrower than in the previous one. Thus the output signal values are more concentrated around -1 and +1 respectively. This leads to lower error level at the decoder output.

The approximated probability density functions of output signal at values of the roll-off factor 0.5 and the relative window width 6 are shown in Fig.5.

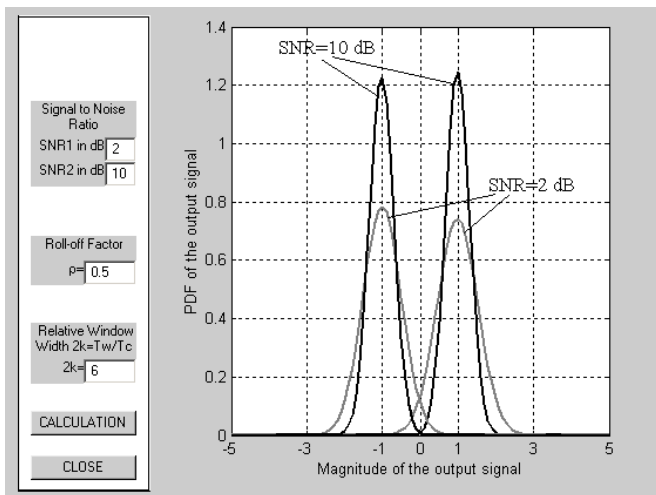


Fig.5. PDF of the output signal at  $\rho=0.5$  and  $2k=6$ .

Fig.5 shows that the mean values of probability density functions are closer to -1 and +1 respectively in comparison with the previous case. The variances of probability density functions are smaller and consequently the probability of error is lower.

The distributions of the output signal at values of 0.4 and 9 for the roll-off factor and the relative window width respectively are shown in Fig.6.

The comparison between these distributions of the output signal and previous distributions shows that they are wider than these at the roll-off factor 0.5 and the relative window width 6, but they slightly differ from those ones at the roll-off factor 1 and the relative window width 3. This is a result from windowing of the impulse responses of the shaping and matched filters in the transmitter and the receiver respectively [2].

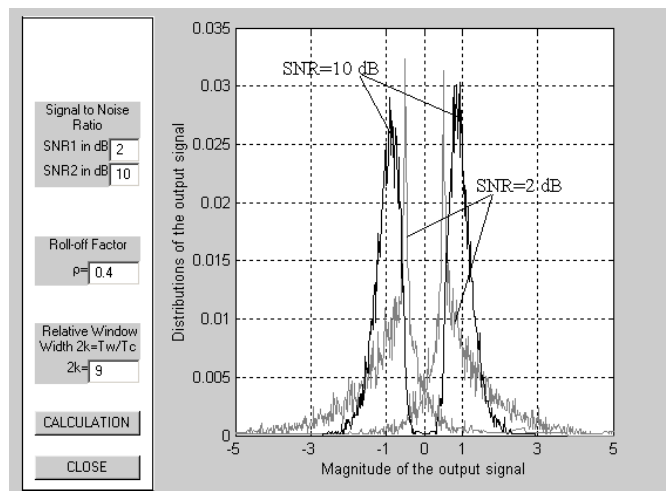


Fig.6. Distributions of the output signal at  $\rho=0.4$  and  $2k=9$ .

The approximated probability density functions of output signal at values of the roll-off factor 0.4 and the relative window width 9 are shown in Fig.7.

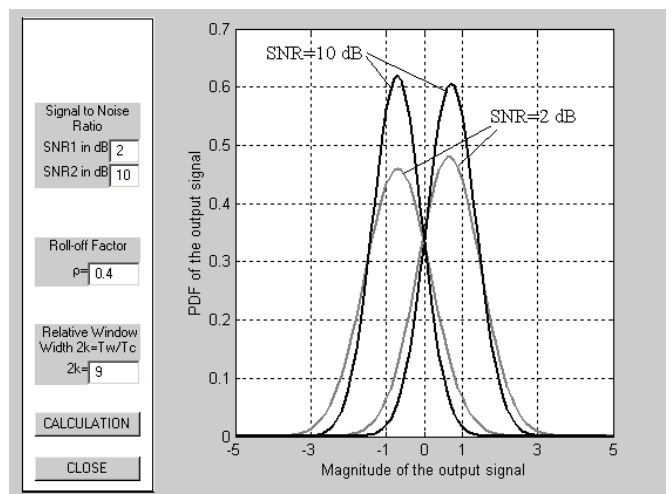


Fig.7. PDF of the output signal at  $\rho=0.4$  and  $2k=9$ .

The more precise analysis of the results indicates that the approximated probability density functions in Fig.7 are narrower than these in Fig.3. This means that the error levels are lower at cases displayed in Fig.6 and Fig.7 than these displayed in Fig.2 and Fig.3, but the differences between them are too small. A conclusion that the even number of the relative window width leads to lower error level than cases of odd such number can be done. The results shown in the following figures confirm this inference.

The distributions of the output signal at values of 0.4 and 4 for the roll-off factor and the relative window width respectively are shown in Fig.8.

tively are shown in Fig.8. It is obvious that these distributions are more concentrated around -1 and +1 respectively than those in Fig.6. This leads to narrower probability density functions and consequently to lower error levels.

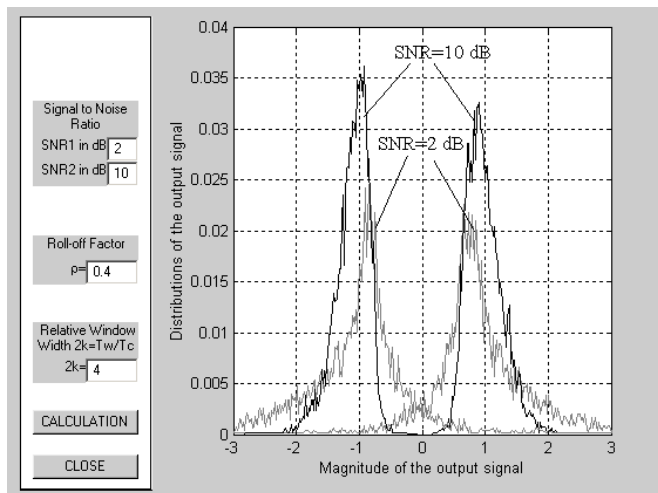


Fig.8. Distribution of the output signal at  $\rho=0.4$  and  $2k=4$ .

The approximated probability density functions of the output signal at values of the roll-off factor 0.4 and the relative window width 4 are shown in Fig.9.

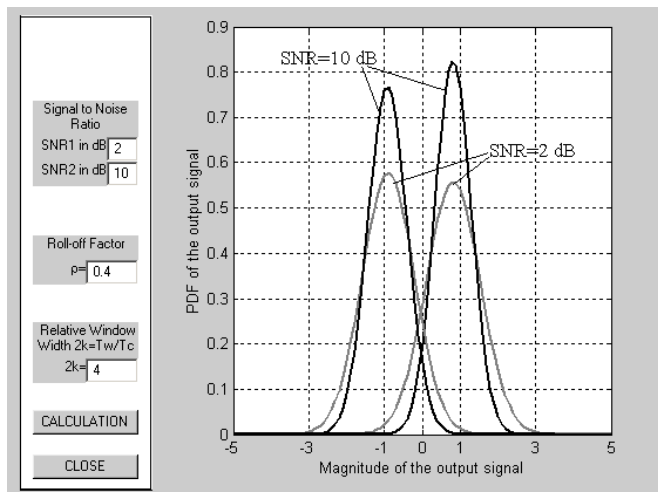


Fig.9. PDF of the output signal at  $\rho=0.4$  and  $2k=4$ .

It is easy to find that if +1 is transmitted, the area under this part of the probability density function where the output signal magnitude is below 0, is much smaller than in the case shown in Fig.7. The same one is valid for the part of probability function where the output signal magnitude exceeds 0 when -1 is transmitted. The value of PDF at output signal magnitude 0 and SNR 10 dB in Fig.9 is below 0.2, while the corresponding PDF in Fig.7 exceeds 0.3 i.e. it is almost twice greater. Furthermore it is obvious that the values of PDF at output signal magnitudes -1 and +1 in Fig.9 are higher than these in Fig.7.

The probability of error can be calculated by obtained quantities of the mean values and the variances and Eq.6:

$$P_{\text{err}} = 1 - \frac{1}{2} \left[ \text{erf} \left( \frac{-m_2}{\sqrt{2}\sigma_2} \right) - \text{erf} \left( \frac{-m_1}{\sqrt{2}\sigma_1} \right) \right], \quad (10)$$

where  $m_1$  and  $\sigma_1^2$  are the mean value and the variance when +1 is transmitted;  $m_2$  and  $\sigma_2^2$  are the mean value and the variance when -1 is transmitted.

The examination of the error probability as a function of SNR at different combinations of the roll-off factor and the relative window width values is done, too. Some of the obtained results are shown in Fig.10.

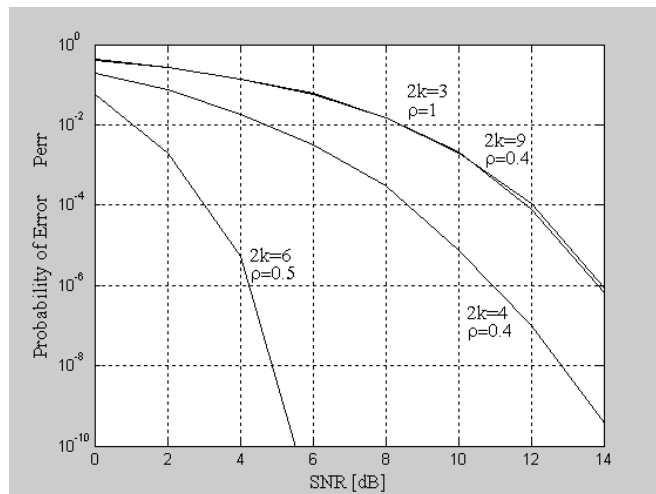


Fig.10. Probability of error as a function of SNR.

It is obvious from the results that the behavior of the probability of error at the parameter pairs  $2k=3$ ,  $\rho=1$  and  $2k=9$ ,  $\rho=0.4$  is the same. The steepest slope of the function is at pair  $2k=6$ ,  $\rho=0.5$  and very likely this is the optimal parameter pair.

#### IV. CONCLUSION

The studies of the differential BPSK decoder show that it possesses good characteristics in the presence of additive white Gaussian noise. It is better an even value of the relative window width to be used. Thus the lower error probability is provided in comparison with the case of an odd value. The results display that for even value the error probability decreases when the relative window width increases. The decoder provides the error probability below  $10^{-6}$  when SNR exceeds 14 dB in the worst case. Obtained results prove that the practical development of such decoder is useful.

The recommendations in [2] should be kept in mind when the decoder parameters are chosen. Detailed studies and analysis of the influence of different factors and parameters should be done during development of a practical scheme of the pair encoder/decoder. Thus the best parameters can be chosen and the best results can be reached.

#### REFERENCES

- [1] G. Stanchev, *Doctoral thesis: Study of Satellite Digital Communication System Stability, Using Spread Spectrum Signals*, Dolna Mitroplia, 2000.
- [2] G. Stanchev, M. Marinov. *Model of a Differential BPSK Decoder with Matched Filter Included, Providing a Minimal ISI*, ICEST 2004, Conference Proceedings, Bitola, Macedonia 2004.
- [3] *Handbook of Mathematical Functions*, edited by Milton Abramowitz and Irene A. Stegun, Moscow, 1979.